DISTRIBUTED CONTROL OF TWO DIMENSIONAL VEHICULAR FORMATIONS: STABILITY MARGIN IMPROVEMENT BY MISTUNING

He Hao **Prabir Barooah** * **Prashant G. Mehta**

ABSTRACT

We consider distributed control of a large two-dimensional (planar) vehicular formation. An individual vehicle in the formation is assumed to be a fully actuated point mass. The control objective is to move the formation with a constant pre-specified velocity while maintaining constant inter-vehicle separation between any pair of nearby vehicles. The control law is distributed in the sense that the control action at each vehicle depends on the relative position measurements with nearby vehicles and its own velocity measurement. For this problem, a partial differential equation (PDE) model is derived to describe the spatio-temporal evolution of velocity perturbations for large number of vehicles, N_{veh}. The PDE model is used to deduce asymptotic formulae for the stability margin (absolute value of the real part of the least stable eigenvalue). We show that the stability margin of the closed loop decays to 0 as the number of vehicles increases, but the decay rate in 2D formation is much slower than in 1D platoons. In addition, the PDE is used to optimize the stability margin using a mistuning-based approach, in which the control gains of the vehicles are changed slightly from their nominal values. We show that the mistuning design reduces the loss of stability margin significantly even with arbitrarily small amount of mistuning. The results of the analysis with the PDE model are corroborated with numerical computation of eigenvalues with the state-space model of the vehicular formation.

1 Introduction

We consider the problem of controlling a large two-dimensional (planar) formation of vehicles so that the group of vehicles move with a constant pre-specified velocity while neighboring vehicles maintain a constant pre-specified spacing. The control law is distributed in the sense that the control action at each vehicle depends on the relative position measurements with nearby vehicles (four nearest neighbors in the plane) and its own velocity measurement. The desired spacings between nearby vehicles and the desired velocity of the formation are assumed to be known to every vehicle. This problem is relevant to a number of applications such as formation flying of aerial, ground, and autonomous vehicles for surveillance, reconnaissance, minesweeping, etc. [1–3]. In many of these applications where the number of vehicles is large, a centralized control solution with its large communication requirements is practically infeasible. This motivates distributed control architectures that is the focus of this paper.

Although distributed control of two and three-dimensional formations arise in a number of applications [3], much research has focused only on one-dimensional problems [4, 5]. For such problems, a number of papers show that distributed control suffers from several challenges for large number of vehicles: First, the least stable closed-loop eigenvalue approaches zero as the number of vehicles, N_{veh}, increases [6, 7]. This progressive loss of closed-loop damping causes the closed loop performance of the platoon to become arbitrarily sluggish as the number of vehicles gets large. Second, with decentralized control the sensitivity of the closed loop system to external disturbances increases with N_{veh} [8–11]. Third, there is a lack of design methods for distributed architectures. For N_{veh} vehicles, in general, N_{veh} distinct controllers need to be designed, for which few control design methods exist. This has led to the examination of only the symmetric control among bidirectional architectures [8–10]. Some symmetry aided simplifications are possible for analysis and design in this case.

The issues that arise in the distributed control of vehicle formations in two or three dimensions may be different from those

*Address all correspondence to this author. He Hao and Prabir Barooah are with the Department of Mechanical and Aerospace Engineering, University of Florida, Gainesville, FL 32611. Email: {hehao,pbarooah}@ufl.edu. Prashant G. Mehta is with the Coordinated Science Laboratory, Department of Mechanical Science and Engineering, University of Illinois, Urbana-Champaign, IL 61801. Email: mehtapg@uiuc.edu

in 1D platoons. For example, with a network of first-order dynamic agents, stability of a formation depends on a certain eigenvalue of the graph describing the network [12]. This eigenvalue may differ significantly depending on whether the graph is 1D, 2D, or 3D [13]. However, the effect of dimension on distributed control of a network of second order agents has not been investigated thoroughly. In a recent paper [14], Bamieh *et. al.* examined d-dimensional vehicle formation with distributed symmetric control law, i.e., where all vehicles using the same control gains. They showed that the long-range coherence of the formation depends crucially on the dimension d.

In this paper we describe a methodology for analysis and distributed feedback control of two-dimensional vehicular formations. The centerpiece of the methodology is a partial differential equation (PDE) approximation that is used to describe the evolution of velocity perturbations in a large two-dimensional (planar) vehicular formation. By building on our earlier work for one-dimensional platoon in [7]), we use the PDE model to obtain results on both analysis and mistuning-based distributed control design for two-dimensional formations.

There are two contributions of this paper: First, we provide an asymptotic formula for the stability margin of a two-dimensional rectangular formation. The formula shows that with a distributed symmetric control, the least stable eigenvalue approaches zero as $O(\frac{1}{N_{\text{veh}}})$ as $N_{\text{veh}} \to \infty$. The formula is verified using numerical computation of the eigenvalues with the state space model of the formation. The asymptotic formula has some interesting implications on the stability margin comparison between one-dimensional and two-dimensional formations. For one-dimensional formations (i.e., platoons), the least stable eigenvalue approaches 0 as $O(\frac{1}{N_{\text{veh}}^2})$ [7]. Even for a moderate number of vehicles, $\frac{1}{N_{\text{veh}}^2} << \frac{1}{N_{\text{veh}}}$. Thus, by arranging the same number of vehicles in a two-dimensional formation instead of a one-dimensional platoon, the stability margin can be improved significantly (with the same control gains).

The second contribution is a *mistuning*-based design of control gains - which is naturally suggested by the PDE model – in which the gains are perturbed from their nominal values by a small amount. We show that an arbitrarily small perturbation (asymmetry) in the controller gains from their nominal (symmetric) value can improve the closed-loop stability margin. In particular, the least stable eigenvalue of the 2D formation approaches 0 as $O(\frac{1}{\sqrt{N_{\text{veh}}}})$. Thus, even for moderate number of vehicles, a small amount of mistuning can lead to significant improvement in the closed loop stability margin, from $O(\frac{1}{N_{\text{veh}}})$ to $O(\frac{1}{\sqrt{N_{\text{veh}}}})$. The optimal mistuning profile is determined by using a perturbation procedure.

The restriction to two-dimensions in this paper is made primarily for ease of notation and lucid presentation of main ideas. All the ideas can be extended to 3D formations in a straightforward manner. Although the results in this paper are given only for two-dimensional formations, extensions to three-dimensions can be carried out in a straightforward manner.

The remainder of this paper is organized as follows. Section 2 describes the discrete and continuous models of the formation control problem. Analysis and control design results together with their numerical verification appear in Sections 3 and 4, respectively. The paper ends with conclusions and suggestions for future research in Section 5.

2 Closed loop dynamics of 2D vehicular formation

In this section, we derive the closed loop dynamics of a 2D formation of vehicles with distributed control. We first present the state-space model of the closed loop system, and then derive the PDE model of the same under the continuum approximation.

2.1 State-space model of controlled formation

Consider a rectangular formation of $L \times M$ identical vehicles moving in a plane, as shown in Fig. 1 (see also Fig. 2). Let $P_{(i,j)}(t) := [X_{(i,j)}(t), Y_{(i,j)}(t)]^T \in \mathbb{R}^2$ denote the position and $V_{(i,j)}(t) := \dot{P}_{(i,j)}(t)$ denote the velocity of the $(i,j)^{\text{th}}$ vehicle, for $i = 1 \dots L, j = 1 \dots M$. The dynamics of each vehicle is modeled as a double integrator:

$$\ddot{P}_{(i,j)}(t) = U_{(i,j)}, \tag{1}$$

where $U_{(i,j)} = [U_{X,(i,j)}, U_{Y,(i,j)}]^T \in \mathbb{R}^2$ is the control applied to the $(i,j)^{\text{th}}$ vehicle. The control objective is to maintain a constant spacing between each vehicle and their nearest neighbors ($\Delta_X \in \mathbb{R}$ in the X-direction and $\Delta_Y \in \mathbb{R}$ in the Y-direction) and a constant desired velocity ($V^d := [V_X^d, V_Y^d]^T \in \mathbb{R}^2$). The solid dots in Fig. 1 represent the desired positions of the vehicles in a coordinate system that is moving at a constant velocity V^d.

For ease of description, we refer to the positive X-direction as *East*(E), negative X-direction as *West*(W), positive Y-direction as *North*(N), and negative Y-direction as *South*(S) (see Fig. 1). Following the formulation used in [6, 7] for 1D platoons, we introduce fictitious reference vehicles on the four (E,W,N,S) boundaries of the 2-D formation: $(i,0), (0,j), (i,M+1), (L+1,j)$, where $i = 0,1,\cdots,L$ and $j = 1,2,\cdots,M$. The control objective for the $(i,j)^{\text{th}}$ vehicle is to follow the reference trajectory:

$$P_{i,j}^d := V^d t + \begin{bmatrix} H_X - i\Delta_X \\ H_Y - j\Delta_y \end{bmatrix}, \tag{2}$$

where $H_X := (L+1)\Delta_X$ and $H_Y := (M+1)\Delta_Y$ are the length and width of the formation including the fictitious lead vehicles (Figure 1). The fictitious vehicles' trajectories satisfy $P_{(i,j)}(t) = P^d(i,j)(t)$ for $i = 0, j = 0, \dots, M+1$, and for $j = 0, i = 0, \dots, N+1$.

In this paper we consider a distributed control law such that the control $U_{(i,j)}$ for the $(i,j)^{\text{th}}$ vehicle depends only on the relative position with its four nearest neighbors (i.e., $(i-1,j)^{\text{th}}$, $(i+1,j)^{\text{th}}$, $(i,j-1)^{\text{th}}$, $(i,j+1)^{\text{th}}$) and the desired velocity $V^d := [V_X^d, V_Y^d]^T$. The control law is expressed as

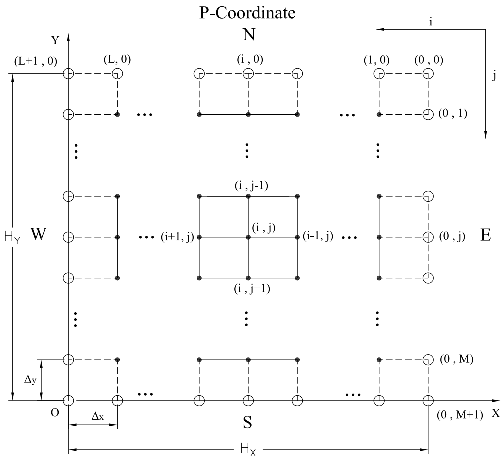

Figure 1. A 2D VEHICULAR FORMATION WITH $L\times M$ VEHICLES; EACH GRID POINT IS A DESIRED POSITION OF A VEHICLE IN A CARTESIAN REFERENCE FRAME THAT IS MOVING AT A CONSTANT VELOCITY OF V_d. THE VEHICLES ON THE BOUNDARY ARE FICTITIOUS REFERENCE VEHICLES.

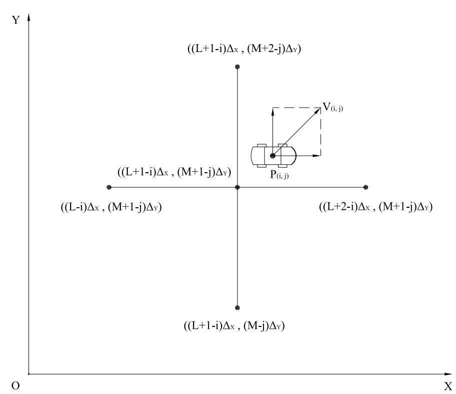

Figure 2. THE POSITION AND VELOCITY OF THE $(i,j)^{\text{TH}}$ VEHICLE.

$$
\begin{aligned}
U_{(i,j)} = {} & K^{(E)}_{(i,j)}(P_{(i,j)} - P_{(i-1,j)} - \Delta_E) + K^{(W)}_{(i,j)}(P_{(i,j)} - P_{(i+1,j)} - \Delta_W) \\
& + K^{(N)}_{(i,j)}(P_{(i,j)} - P_{(i,j-1)} - \Delta_N) + K^{(S)}_{(i,j)}(P_{(i,j)} - P_{(i,j+1)} - \Delta_S) \\
& + K^{(V)}_{(i,j)}(V_{(i,j)} - V^d),
\end{aligned}
\tag{3}
$$

where $\Delta_E = \begin{bmatrix} -\Delta_X \\ 0 \end{bmatrix}$, $\Delta_W = \begin{bmatrix} \Delta_X \\ 0 \end{bmatrix}$, $\Delta_N = \begin{bmatrix} 0 \\ -\Delta_Y \end{bmatrix}$, $\Delta_S = \begin{bmatrix} 0 \\ \Delta_Y \end{bmatrix}$. and $K^{(.)}_{(i,j)}$ is a diagonal gain matrix $K^{(.)}_{(i,j)} := \text{diag}(k^{(.)}_{X,(i,j)}, k^{(.)}_{Y,(i,j)})$, where $k_{X,(i,j)}$ and $k_{Y,(i,j)}$ are negative scalars. The control law is effectively a PD control law: $K^{(E)}_{(i,j)}$, $K^{(W)}_{(i,j)}$, $K^{(N)}_{(i,j)}$ and $K^{(S)}_{(i,j)}$ are the *proportional* gains used by the $(i,j)^{\text{th}}$ vehicle on the relative position errors with respect to its four neighbors – East, West, North and South, respectively, and $K^{(V)}_{(i,j)}$ is the *derivative* gain.

To facilitate representation of the closed-loop dynamics in a way that makes discussion of stability easier, we define the position and velocity error states for each vehicle:

$$
\tilde{p}_{(i,j)}(t) := S\left(P_{(i,j)} - P^d_{(i,j)}\right), \quad \tilde{v}_{(i,j)}(t) := S\left(V_{(i,j)} - V^d_{(i,j)}\right), \tag{4}
$$

where $S = \text{diag}(2\pi/H_X, 2\pi/H_Y)$. With these definitions, the dynamics of the $(i,j)^{\text{th}}$ vehicle are given by

$$
\begin{aligned}
\ddot{\tilde{p}}_{(i,j)} - K^{(V)}_{(i,j)}\tilde{v}_{(i,j)} = {} & K^{(E)}_{(i,j)}(\tilde{p}_{(i,j)} - \tilde{p}_{(i-1,j)}) + K^{(W)}_{(i,j)}(\tilde{p}_{(i,j)} - \tilde{p}_{(i+1,j)}) \\
& + K^{(N)}_{(i,j)}(\tilde{p}_{(i,j)} - \tilde{p}_{(i,j-1)}) + K^{(S)}_{(i,j)}(\tilde{p}_{(i,j)} - \tilde{p}_{(i,j+1)})
\end{aligned}
\tag{5}
$$

We stack the error states in two tall vectors:

$$
\begin{aligned}
\tilde{\mathbf{P}} &:= [\tilde{p}_{(1,1)}, \tilde{p}_{(2,1)}, \cdots, \tilde{p}_{(L,1)}, \tilde{p}_{(1,2)}, \tilde{p}_{(2,2)}, \cdots, \tilde{p}_{(L,2)}, \cdots, \tilde{p}_{(L,M)}]^T \\
\tilde{\mathbf{V}} &:= \dot{\tilde{\mathbf{P}}} = [\tilde{v}_{(1,1)}, \tilde{v}_{(2,1)}, \cdots, \tilde{v}_{(L,1)}, \tilde{v}_{(1,2)}, \tilde{v}_{(2,2)}, \cdots, \tilde{v}_{(L,M)}]^T
\end{aligned}
$$

It follows from straightforward algebraic manipulation that the state-space model of the vehicle formation can now be written compactly as:

$$
\begin{bmatrix} \dot{\tilde{\mathbf{P}}} \\ \dot{\tilde{\mathbf{V}}} \end{bmatrix} = \mathbf{A} \begin{bmatrix} \tilde{\mathbf{P}} \\ \tilde{\mathbf{V}} \end{bmatrix} \tag{6}
$$

where the closed-loop dynamics matrix $\mathbf{A}$ is described in Appendix.

Our goal is to analyze the closed-loop stability margin with increasing L, M and to devise ways to improve it by appropriately choosing the controller gains. While in principle this can be done by analyzing the eigenvalues of the matrix $\mathbf{A}$, we take an alternate route. For large values of L and M, we approximate the dynamics of the discrete formation by a partial differential equation (PDE) which is used for analysis and control design.

2.2 Continuous model of closed loop formation dynamics

To derive the PDE approximation, we first differentiate Equation (5) with respect to time,

$$
\begin{aligned}
\ddot{\tilde{v}}_{(i,j)} - K^{(V)}_{(i,j)}\dot{\tilde{v}}_{(i,j)} = {} & K^{(E)}_{(i,j)}(\tilde{v}_{(i,j)} - \tilde{v}_{(i-1,j)}) + K^{(W)}_{(i,j)}(\tilde{v}_{(i,j)} - \tilde{v}_{(i+1,j)}) \\
& + K^{(N)}_{(i,j)}(\tilde{v}_{(i,j)} - \tilde{v}_{(i,j-1)}) + K^{(S)}_{(i,j)}(\tilde{v}_{(i,j)} - \tilde{v}_{(i,j+1)}).
\end{aligned}
$$

Denoting $K^{X(+)}_{(i,j)} = K^{(E)}_{(i,j)} + K^{(W)}_{(i,j)}$, $K^{X(-)}_{(i,j)} = K^{(E)}_{(i,j)} - K^{(W)}_{(i,j)}$, $K^{Y(+)}_{(i,j)} = K^{(N)}_{(i,j)} + K^{(S)}_{(i,j)}$, and $K^{Y(-)}_{(i,j)} = K^{(N)}_{(i,j)} - K^{(S)}_{(i,j)}$, we have

$$\begin{aligned}\ddot{\tilde{v}}_{(i,j)} - K^{(V)}_{(i,j)}\dot{\tilde{v}}_{(i,j)} &= K^{X(+)}_{(i,j)}\tilde{v}_{(i,j)} + K^{Y(+)}_{(i,j)}\tilde{v}_{(i,j)} \\ &- \frac{K^{X(+)}_{(i,j)} + K^{X(-)}_{(i,j)}}{2}\tilde{v}_{(i-1,j)} - \frac{K^{X(+)}_{(i,j)} - K^{X(-)}_{(i,j)}}{2}\tilde{v}_{(i+1,j)} \\ &- \frac{K^{Y(+)}_{(i,j)} + K^{Y(-)}_{(i,j)}}{2}\tilde{v}_{(i,j-1)} - \frac{K^{Y(+)}_{(i,j)} - K^{Y(-)}_{(i,j)}}{2}\tilde{v}_{(i,j+1)}. \qquad (7)\end{aligned}$$

To facilitate the PDE derivation, we introduce a coordinate transformation so that the position of every vehicle in the new coordinate lies in $[0,2\pi]$ irrespective of the number of vehicles:

$$p_{(i,j)}(t) := \begin{bmatrix} \frac{2\pi}{H_X}\left(X_{(i,j)}(t) - V^d_X t\right) \\ \frac{2\pi}{H_Y}\left(Y_{(i,j)}(t) - V^d_Y t\right)\end{bmatrix}, \quad v_{(i,j)}(t) = \begin{bmatrix}\frac{2\pi}{H_X}V_{X,(i,j)} \\ \frac{2\pi}{H_Y}V_{Y,(i,j)}\end{bmatrix}.$$

The desired spacing and velocity in the transformed coordinates are $[\delta_x,\ \delta_y]^T = S[\Delta_X,\ \Delta_Y]^T$ and $v^d := S(V^d - V^d) = 0$, where $S := \text{diag}(2\pi/H_X, 2\pi/H_Y) \in \mathbb{R}^{2\times 2}$. The desired position of the $(i,j)^{\text{th}}$ vehicle becomes $p^d_{(i,j)}(t) = \text{diag}(L+1-i, M+1-j)[\delta_x, \delta_y]^T$. After some manipulations, Eq. (7) can be expressed as

$$\begin{aligned}\ddot{\tilde{v}}_{(i,j)} - K^{(V)}_{(i,j)}\dot{\tilde{v}}_{(i,j)} = &-\delta_x K^{X(-)}_{(i,j)}\frac{\tilde{v}_{(i-1,j)} - \tilde{v}_{(i+1,j)}}{2\delta_x} \\ &- \delta_x^2\frac{K^{X(+)}_{(i,j)}}{2}\frac{\tilde{v}_{(i-1,j)} - 2\tilde{v}_{(i,j)} + \tilde{v}_{(i+1,j)}}{\delta_x^2} \\ &- \delta_y K^{Y(-)}_{(i,j)}\frac{\tilde{v}_{(i,j-1)} - \tilde{v}_{(i,j+1)}}{2\delta_y} \\ &- \delta_y^2\frac{K^{X(+)}_{(i,j)}}{2}\frac{\tilde{v}_{(i-1,j)} - 2\tilde{v}_{(i,j)} + \tilde{v}_{(i+1,j)}}{\delta_y^2}. \qquad (8)\end{aligned}$$

We now introduce a vector function $\tilde{v}(x,y,t) : [0,2\pi]\times[0,2\pi]\times[0,\infty) \to \mathbb{R}^2$ that will serve as a continuous approximation of the velocities $\tilde{v}_{i,j}$ by the following stipulation:

$$\tilde{v}_{i,j}(t) = \tilde{v}(x,y,t)|_{[x,y]=p_{(i,j)}}.$$

To write a PDE model from (8), we use the following finite difference approximations:

$$\left[\frac{\tilde{v}_{(i-1,j)} - \tilde{v}_{(i+1,j)}}{2\delta_x}\right] = \left[\frac{\partial\tilde{v}(x,y,t)}{\partial x}\right]_{[x,y]=p_{(i,j)}},$$
$$\left[\frac{\tilde{v}_{(i-1,j)} - 2\tilde{v}_{(i,j)} + \tilde{v}_{(i+1,j)}}{\delta_x^2}\right] = \left[\frac{\partial^2\tilde{v}(x,y,t)}{\partial x^2}\right]_{[x,y]=p_{(i,j)}},$$
$$\left[\frac{\tilde{v}_{(i,j-1)} - \tilde{v}_{(i,j+1)}}{2\delta_y}\right] = \left[\frac{\partial\tilde{v}(x,y,t)}{\partial y}\right]_{[x,y]=p_{(i,j)}},$$
$$\left[\frac{\tilde{v}_{(i,j-1)} - 2\tilde{v}_{(i,j)} + \tilde{v}_{(i,j+1)}}{\delta_y^2}\right] = \left[\frac{\partial^2\tilde{v}(x,y,t)}{\partial y^2}\right]_{(x,y)=p_{(i,j)}}.$$

The matrix functions $K^{(E)}, K^{(W)}, K^{(N)}, K^{(S)}, K^{(V)} : \mathbb{R}^2 \to \mathbb{R}^{2\times 2}$ are used to write continuous approximations of the gains with the stipulation:

$$K^{(\cdot)}_{i,j} = K^{(\cdot)}(x,y)|_{[x,y]=p_{(i,j)}}.$$

Using these functions, $K^{X(+)} := K^{(E)}(x,y) + K^{(W)}(x,y)$, $K^{X(-)} := K^{(E)}(x,y) - K^{(W)}(x,y)$, $K^{Y(+)} := K^{(N)}(x,y) + K^{(S)}(x,y)$, and $K^{Y(-)} := K^{(N)}(x,y) - K^{(S)}(x,y)$. Equation (8) now becomes:

$$\begin{aligned}&\left(\frac{\partial^2}{\partial t^2} - K^{(V)}(x,y)\frac{\partial}{\partial t}\right)\tilde{v}(x,y,t) \\ &\quad = \Big(-\frac{K^{X(-)}(x,y)}{\rho_x}\frac{\partial}{\partial x} - \frac{K^{X(+)}(x,y)}{2\rho_x^2}\frac{\partial^2}{\partial x^2} \\ &\qquad -\frac{K^{Y(-)}(x,y)}{\rho_y}\frac{\partial}{\partial y} - \frac{K^{Y(+)}(x,y)}{2\rho_y^2}\frac{\partial^2}{\partial y^2}\Big)\tilde{v}(x,y,t), \qquad (9)\end{aligned}$$

where $\rho_x = \frac{1}{\delta_x}$ and $\rho_y = \frac{1}{\delta_y}$ have the physical interpretation of the *mean density* (vehicles per unit length) in the X (i.e., E-W) and Y (i.e., N-S) directions, respectively. With fictitious reference vehicles on all four boundaries, the appropriate boundary condition for the above PDE is of Dirichlet type:

$$\tilde{v}(0,y,t) = \tilde{v}(2\pi,y,t) = \tilde{v}(x,0,t) = \tilde{v}(x,2\pi,t) = 0. \qquad (10)$$

Note that $\tilde{v}(x,y,t)$ in the above PDE (9) has two components, which we call φ and ψ: $\tilde{v}(x,y,t) := [\varphi(x,y,t),\ \psi(x,y,t)]^T$. Since the functions $K^{X(+)}, K^{X(-)}$, etc. are all diagonal, the PDE (9) comprises of two scalar PDEs. In particular, let $K^{X(+)} := \text{diag}(k_x^{X(+)}, k_y^{X(+)})$, $K^{X(-)} := \text{diag}(k_x^{X(-)}, k_y^{X(-)})$, $K^{Y(+)} := \text{diag}(k_x^{Y(+)}, k_y^{Y(+)})$, $K^{Y(-)} := \text{diag}(k_x^{Y(-)}, k_y^{Y(-)})$, $K^{(V)} := \text{diag}(k_x^{(V)}, k_y^{(V)})$ and define the linear operators $\mathcal{L}_x$ and $\mathcal{L}_y$ as follows:

$$\begin{aligned}\mathcal{L}_x := \frac{1}{2\rho_x}k_x^{X(-)}(x,y)\frac{\partial}{\partial x} + \frac{1}{2\rho_x^2}k_x^{X(+)}(x,y)\frac{\partial^2}{\partial x^2} + \\ \frac{1}{2\rho_y}k_x^{Y(-)}(x,y)\frac{\partial}{\partial y} + \frac{1}{2\rho_y^2}k_x^{Y(+)}(x,y)\frac{\partial^2}{\partial y^2}\end{aligned}$$

and $\mathcal{L}_y$ is obtained by replacing $k_x^{(\cdot)}$ in $\mathcal{L}_x$ by $k_y^{(\cdot)}$. The PDE (9) becomes

$$\left(\frac{\partial^2}{\partial t^2} - k_x^{(V)}(x,y)\frac{\partial}{\partial t} + \mathcal{L}_x\right)\varphi = 0, \qquad (11)$$

$$\left(\frac{\partial^2}{\partial t^2} - k_y^{(V)}(x,y)\frac{\partial}{\partial t} + \mathcal{L}_y\right)\psi = 0, \tag{12}$$

subject to the following boundary conditions:

$$\varphi(0,y,t) = \varphi(2\pi,y,t) = \varphi(x,0,t) = \varphi(x,2\pi,t) = 0, \tag{13}$$
$$\psi(0,y,t) = \psi(2\pi,y,t) = \psi(x,0,t) = \psi(x,2\pi,t) = 0. \tag{14}$$

2.3 Comparison of eigenvalue between SSM and PDE

For preliminary validation of the PDE model, we compare the closed loop eigenvalues predicted by the the state-space and the PDE models for symmetric control, in which a vehicle uses the same control gains on all the four directions E,W,N,S and every vehicle uses the same gains: $k^{(E)}(x,y) = k^{(W)}(x,y) = k^{(N)}(x,y) = k^{(S)}(x,y) = -k_0 I$, and $k^{(V)}(x,y) = -b_0 I$, where k_0 and b_0 are constant positive numbers. In that case, $k_x^{X(-)}(x,y) = 0$ and $k_x^{X(+)}(x,y) = -2k_0$, and the PDE (11) simplifies to:

$$\left(\frac{\partial^2}{\partial t^2} + b_0\frac{\partial}{\partial t} - \mathcal{L}_0(x,y)\right)\varphi(x,y,t) = 0, \tag{15}$$

where

$$\mathcal{L}_0(x,y) := a_x^2\frac{\partial^2}{\partial x^2} + a_y^2\frac{\partial^2}{\partial y^2} \tag{16}$$

is a Laplacian operator and $a_x^2 := k_0\delta_x^2$, $a_y^2 := k_0\delta_y^2$ are the wave speeds in the x and y direction respectively. With symmetric control, the PDEs (11) and (12) are the same, so we need to examine only one.

Figure 3 shows the closed-loop eigenvalues obtained using the state-space model (eigenvalues of $\mathbf{A}$ in Eq. 6) and those obtained using the PDE (15), for a 10×10 vehicular formation. The PDE eigenvalues are computed by using a Galerkin projection method. The figure shows that the eigenvalues of the SSM (State-Space Model) and PDE model match very well, especially for the least stable eigenvalue (eigenvalue closest to the imaginary axis).

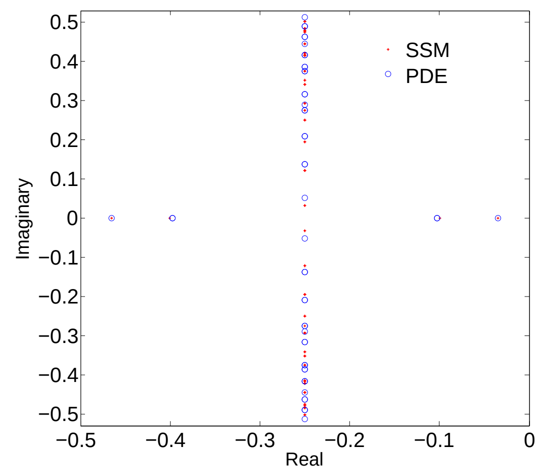

Figure 3. COMPARISON OF CLOSED-LOOP EIGENVALUES PREDICTED BY THE STATE-SPACE MODEL (SSM) AND PDE MODEL OF A 10×10 2-D VEHICULAR FORMATION WITH SYMMETRIC CONTROL. THE GAINS USED ARE $k_0 = 0.1$ AND $b_0 = 0.5$. THIS MEANS THAT FOR THE STATE-SPACE MODEL (6), $K_{(i,j)}^{(E,W,N,S)} = -0.1\,I$, $K^{(V)} = -0.5I$. ONLY A FEW OF EIGENVALUES ARE COMPARED IN THE FIGURE.

3 Analysis of stability margin

After taking a Laplace transform of the PDE (15) with respect to the time variable t, (with s as the Laplace variable), the eigenvalues of the PDE (15) are the values of s that satisfy

$$s^2 + b_0 s + \lambda = 0, \tag{17}$$

where λ is an eigenvalue of the Laplacian operator $\mathcal{L}_0(x,y)$ (see (16)). The eigenvalues are therefore given by

$$s_{(\ell,m)}^{\pm} = \frac{-b_0 \pm \sqrt{b_0^2 - 4\lambda}}{2}. \tag{18}$$

For Dirichlet boundary conditions on a rectangular domain, $\lambda = \left(\frac{\ell}{2}\right)^2 a_x^2 + \left(\frac{m}{2}\right)^2 a_y^2$, for $\ell = 1,2,\cdots,\infty$, $m = 1,2,\cdots,\infty$. For a fixed ℓ and m, there are two eigenvalues in formula (18). The one closer to the imaginary axis is denoted by $s_{(\ell,m)}^{+}$, and the other, by $s_{(\ell,m)}^{-}$. We call $s_{(\ell,m)}^{+}$ the *less stable* eigenvalue. The next Lemma describes the dependence of these eigenvalues on L and M, the number of vehicles in the E-W and N-S directions.

Lemma 1. *Consider the eigenvalue problem for the linear PDE* (15) *with Dirichlet boundary conditions (13). The* $(l,m)^{th}$ *less-stable eigenvalue* $s_{(l,m)}^{+}$ *approaches* 0 *as* $O(1/L^2) + O(1/M^2)$ *when* $L, M \to \infty$. □

Proof. Using Eq. (18), we have

$$\begin{aligned} 2s_{(l,m)}^{\pm} &= -b_0 \pm b_0\left(1 - \frac{l^2 a_x^2 + m^2 a_y^2}{b_0^2}\right)^{1/2} \\ &= -b_0 \pm b_0\left(1 - \frac{2\pi^2 k_0}{b_0^2}\left(\frac{l^2}{(L+1)^2} + \frac{m^2}{(M+1)^2}\right)\right) \\ &+ O\left(\frac{1}{L^4}\right) + O\left(\frac{1}{M^4}\right) \end{aligned} \tag{19}$$

for large L and M. It follows that

$$s_{(l,m)}^{+} = -\frac{\pi^2 k_0}{b_0}\left(\frac{l^2}{(L+1)^2} + \frac{m^2}{(M+1)^2}\right) + O\left(\frac{1}{L^4}\right) + O\left(\frac{1}{M^4}\right).$$

■

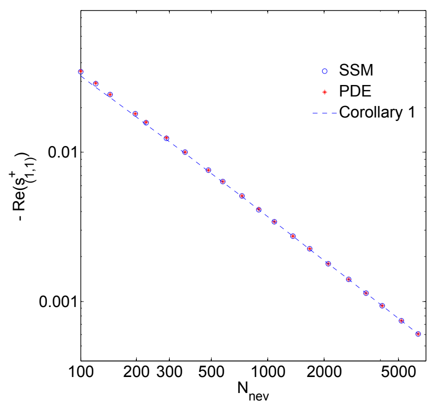

Figure 4. THE LEAST STABLE EIGENVALUE OF THE CLOSED LOOP FORMATION DYNAMICS WITH SYMMETRIC CONTROL ($k_0 = 0.1$ AND $b_0 = 0.5$) AS A FUNCTION OF NUMBER OF VEHICLES: THE PREDICTIONS FROM THE STATE SPACE MODEL (SSM), THE PDE MODEL, AND THE ASYMPTOTIC FORMULA IN COROLLARY 1.

The stability margin of the formation is measured by the real part of $s^+_{(1,1)}$, the *least stable eigenvalue*. The following corollary to Lemma 1 describes the trend of the stability margin as a function of the number of vehicles in a *square* formation (i.e., $L = M$).

Corollary 1. *Consider a square formation of N_{veh} vehicles with symmetric control. The least stable eigenvalue is given by*

$$s^+_{(1,1)} = -\frac{2\pi^2 k_0}{b_0}\frac{1}{(\sqrt{N_{veh}}+1)^2} + O(\frac{1}{N_{veh}^2})$$
$$= -\frac{2\pi^2 k_0}{b_0}\frac{1}{N_{veh}} + O(\frac{1}{N_{veh}^2}). \qquad \square$$

To verify corollary (1), we numerically compute the least stable eigenvalue of the $\mathbf{A}$ matrix in Eq. (6), and also the least stable eigenvalue of the PDE (15). Figure 4 depicts these results showing excellent agreement.

In summary, Corollary 1 shows that the least stable eigenvalue with symmetric control approaches 0 as $O(\frac{1}{N_{\text{veh}}})$ for 2-D square formation ($L = M$), where $N_{\text{veh}} := L^2$ is total number of vehicles in the formation.

4 Reducing loss of stability by mistuning

In this section we introduce a mistuning-based method to change the symmetric gains slightly in order to improve the stability margin.

Due to the decoupled nature of the two PDEs, we consider one at a time. We first introduce small perturbations on the gains:

$$k_x^{(E)}(x,y) = -k_0 - \varepsilon k_x^{(purt,E)}(x,y)$$
$$k_x^{(W)}(x,y) = -k_0 - \varepsilon k_x^{(purt,W)}(x,y)$$
$$k_x^{(N)}(x,y) = -k_0 - \varepsilon k_x^{(purt,N)}(x,y)$$
$$k_x^{(S)}(x,y) = -k_0 - \varepsilon k_x^{(purt,S)}(x,y)$$

where $k_x^{(\cdot)}(x,y) : \mathbb{R}^2 \to R$ is the $(1,1)$ component of the matrix gain function $K^{(\cdot)}(x,y)$, k_0 is the nominal value of the symmetric control gain, $\varepsilon > 0$ is a small positive number that denotes the amount of mistuning and $k^{(purt,.)}(x,y)$ is the perturbation function to be designed. We also have,

$$k_x^{(+)}(x,y) = -2k_0 - \varepsilon k_s^x(x,y),\; k_x^{(-)}(x,y) = -\varepsilon k_m^x(x,y),$$
$$k_y^{(+)}(x,y) = -2k_0 - \varepsilon k_s^y(x,y),\; k_y^{(-)}(x,y) = -\varepsilon k_m^y(x,y),$$

where $k_s^x(x,y) = k^{(purt,E)}(x,y) + k^{(purt,W)}(x,y)$, $k_m^x(x,y) = k^{(purt,E)}(x,y) - k^{(purt,W)}(x,y)$, $k_s^y(x,y) = k^{(purt,N)}(x,y) + k^{(purt,S)}(x,y)$, and $k_m^y(x,y) = k^{(purt,N)}(x,y) - k^{(purt,S)}(x,y)$. Substituting these into PDE (11), we obtain

$$\Big(\frac{\partial^2}{\partial t^2} + b_0\frac{\partial}{\partial t} - a_x^2\frac{\partial^2}{\partial x^2} - a_y^2\frac{\partial^2}{\partial y^2}\Big)\varphi(x,y,t) =$$
$$\varepsilon\Big(\frac{k_m^x}{\rho_x}\frac{\partial}{\partial x} + \frac{k_s^x}{2\rho_x^2}\frac{\partial^2}{\partial x^2} + \frac{k_m^y}{\rho_y}\frac{\partial}{\partial y} + \frac{k_s^y}{2\rho_y^2}\frac{\partial^2}{\partial y^2}\Big)\varphi(x,y,t) \qquad (20)$$

A similar procedure is followed for the PDE (12) that governs the behavior of the y-component of the velocity $\tilde{v}$. We omit that part due to lack of space.

The effect of the perturbations on the symmetric gains on the less stable eigenvalues of the PDE (20) is stated in the next theorem.

Theorem 1. *Consider the eigenvalue problem of the mistuned PDE* (20) *with Dirichlet boundary condition (13). The $(l,m)^{th}$ less stable eigenvalue is given by the following formula:*

$$s^+_{(l,m)}(\varepsilon) =$$
$$\varepsilon\frac{l}{2\pi b_0(L+1)}\int_0^{2\pi}\int_0^{2\pi} k_m^x(x,y)\sin(lx)\sin^2((\frac{m}{2})y)dxdy +$$
$$\varepsilon\frac{m}{2\pi b_0(M+1)}\int_0^{2\pi}\int_0^{2\pi} k_m^y(x,y)\sin^2((\frac{l}{2})x)\sin(my)dxdy +$$
$$+O(\varepsilon^2) + O(\frac{1}{L^2}) + O(\frac{1}{M^2}),$$

that is valid when $\varepsilon \to 0$ and $L, M \to \infty$. $\square$

Proof. The proof is somewhat lengthy, but quite similar to the proof of Theorem 1 in [7], so we only provide a sketch here. The proof proceeds by a perturbation method. Let $\eta(x,y;s)$ be the Laplace transform of $\varphi(x,y,t)$. Let the eigenvalues of the perturbed PDE be $s = s^{(0)} + \varepsilon s^{(\varepsilon)}$, where $s^{(0)}$ is the eigenvalue of the unperturbed PDE, and the subscripts (l,m) are suppressed. Let the corresponding eigenfunctions be $\eta = \eta^{(0)} + \varepsilon\eta^{(\varepsilon)}$. Taking a Laplace transform of both sides of the PDE (20) and plugging in the expressions for s and η, and doing an $O(1)$ balance leads to the eigenvalue equation for the symmetric PDE:

$$\mathcal{P}\eta^{(0)} = 0, \text{ where } \mathcal{P} := \Big((s^{(0)})^2 + b_0 s^{(0)} - a\mathcal{L}\Big) \tag{21}$$

where $a\mathcal{L} := a_x^2 \frac{\partial^2}{\partial x^2} + a_y^2 \frac{\partial^2}{\partial y^2}$. The solution $s^{(0)}, \eta^{(0)}$ to this equation has been previously computed (Lemma 1 describes $s^{(0)}$). Doing an $O(\varepsilon)$ balance leads to the equation

$$\mathcal{P}\eta^{(\varepsilon)} = \Big(-\frac{k_m^x}{\rho_x}\frac{\partial}{\partial x} + \frac{k_s^x}{2\rho_x^2}\frac{\partial^2}{\partial x} - \frac{k_m^y}{\rho_y}\frac{\partial}{\partial y} + \frac{k_s^y}{2\rho_y^2}\frac{\partial^2}{\partial y} - b_0 s^{(\varepsilon)} - 2s^{(0)}s^{(\varepsilon)}\Big)\eta^{(0)} =: R$$

For a solution $\eta^{(\varepsilon)}$ to exist, R must lie in the range space of the operator $\mathcal{P}$. Since $\mathcal{P}$ is self-adjoint, its range space is orthogonal to its null space. Thus, we have

$$< R, \phi_{(l,m)} >= 0 \tag{22}$$

where $\phi_{l,m}$ is the $(l,m)^{\text{th}}$ basis vector of the null space of operator $\mathcal{P}$. Note that $\phi_{(l,m)}$ and $s^{(0)}$ are known from the analysis of the symmetric PDE (15). The result of the Theorem follows from (22) in a straightforward manner. ■

It follows from this theorem that to minimize the least stable eigenvalue, only $k_m^x(x,y)$, $k_m^y(x,y)$ need to be designed carefully, since they have $O(\frac{1}{L})$ and $O(\frac{1}{M})$ effect whereas $k_s^x(x,y)$, $k_s^y(x,y)$ only have a much smaller effect of $O(\frac{1}{L^2})$ and $O(\frac{1}{M^2})$. So we choose $k^{(purt,E)}(x,y) = -k^{(purt,W)}(x,y)$ and $k^{(purt,N)}(x,y) = -k^{(purt,S)}(x,y)$, which results in $k_m^x(x,y) = 2k^{(purt,E)}(x,y)$, $k_s^x(x,y) = 0$ and $k_m^y(x,y) = 2k^{(purt,N)}(x,y)$, $k_s^y(x,y) = 0$. The following corollary gives the optimal perturbation profile $k^{(purt,E)}(x,y)$ and $k^{(purt,N)}(x,y)$ that minimizes the least stable eigenvalue.

Corollary 2. *Consider the problem of minimizing the least-stable eigenvalue of the PDE* (20) *with Dirichlet boundary condition (13) by appropriately choosing* $k^{(purt,E)}(x,y)$, $k^{(purt,N)}(x,y) \in L^\infty([0,2\pi])$ *with the norm-constraint* $\|k^{(purt,E)}(x,y)\|_{L^\infty}, \|k^{(purt,N)}(x,y)\|_{L^\infty} = 1$, *and* $k^{(purt,E)}(x,y) = -k^{(purt,W)}(x,y)$, $k^{(purt,N)}(x,y) = -k^{(purt,S)}(x,y)$. *In the limit as* $\varepsilon \to 0$, *the optimal mistuning profile is given by*

$$k^{(purt,E)}(x,y) = 2(H(x-\pi) - \frac{1}{2}),$$

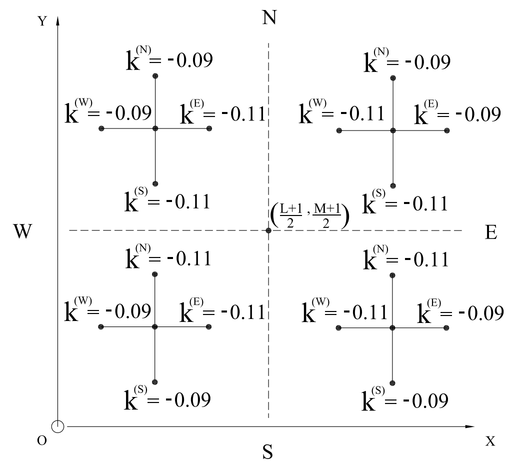

Figure 5. A PICTORIAL REPRESENTATION OF THE x-COMPONENT OF THE GAINS WITH MISTUNED DESIGN. ALL VEHICLES IN THE SAME "QUADRANT" USES THE SAME GAINS.

$$k^{(purt,N)}(x,y) = 2(H(y-\pi) - \frac{1}{2}),$$

where $H(x)$ *is the Heaviside function:* $H(x) = 1$ *for* $x \geq 0$ *and* $H(x) = 0$ *for* $x < 0$.

For a square formation ($M = L$)*, the least stable eigenvalue of PDE* (20) *with the above mistuning profile is*

$$s^{+}_{(1,1)}(\varepsilon) = -\frac{8\varepsilon}{b_0(L+1)} + O(\frac{1}{L^2}) + O(\varepsilon^2)$$
$$= -\frac{8\varepsilon}{b_0}\frac{1}{\sqrt{N_{veh}}} + O(\frac{1}{L^2}) + O(\varepsilon^2)$$

in the limit as $\varepsilon \to 0$ *and* $L = M \to \infty$. □

Figure 5 represent the x-component of the gains, k_x, for the mistuned design, with $\varepsilon = 0.1$. Numerical verification of the mistuning-based control is presented in Figure 6. With $k_0 = 0.1$, $b_0 = 0.5$ and $\varepsilon = 0.01$, the results in Figure 6 show that (i) the mistuning design significantly improves the stability margin over the symmetric design, and (ii) the least stable eigenvalues of mistuned PDE match very well with those of SSM. The mismatch between the numerically computed eigenvalues (PDE or SSM) and the analytical asymptotic formula in Corollary 2 is because of the fact that the formula is valid for only vanishingly small values of ε.

The improvement in the stability margin with mistuning is remarkable since the gains are changed from their nominal symmetric values by only $\pm 10\%$. Another interesting aspect of the result in Corollary 2 is that the improvement from $O(1/N_{\text{veh}})$ to $O(1/\sqrt{N_{\text{veh}}})$ can be achieved by *arbitrarily small changes* to the nominal gains. In addition, the optimal mistuned gain profile is

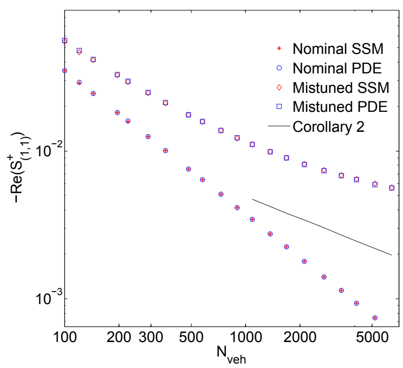

Figure 6. COMPARISON OF THE LEAST STABLE EIGENVALUE OF MISTUNED AND NOMINAL SSM AND PDE.

quite simple to implement - a vehicle only needs to know the amount of mistuning ε, and which "quadrant" of the 2D grid of vehicles it lies in.

5 Conclusion

We have developed a PDE-based continuum approximation of the closed loop dynamics of a 2D formation of vehicles with distributed control. The PDE model facilitates the analysis of closed loop dynamics and also suggests a mistuning based approach for stability improvement. In particular, we showed using the PDE that with symmetric control architecture (every vehicle uses the same control gains), the stability margin - measured by the least stable closed loop eigenvalue – approaches zero as $O(\frac{1}{N_{\text{veh}}})$. The mistuning based approach is used to design the control gains so that with arbitrarily small amount of changes to the gains, the stability margin is improved to $O(\frac{1}{\sqrt{N_{\text{veh}}}})$.

Both of these (analysis and design) are difficult to achieve with the state space model of the dynamics. The results of the analysis with the PDE model are corroborated with numerical computation of eigenvalues with the state-space model of the vehicular formation.

The approach generalizes easily to three-dimensions. In 3D, the least stable eigenvalue with symmetric control approaches zero as $O(1/N_{\text{veh}}^{2/3})$. Using the mistuning based approach, the stability margin can be improved to $O(1/N_{\text{veh}}^{1/3})$. The general d-dimensional case will be discussed in the journal version of this paper. The results of this paper, together with those reported earlier in [7], show that dimension of the network induced by the architecture of distributed control plays a crucial role in determining the closed loop stability margin. In addition, mistuning allows us to improve the performance significantly from the nominal symmetric case.

REFERENCES

[1] Ludwig, P. M., 2000. "Formation control for multi-vehicle robotic minesweeping". Master's thesis, Naval postgraduate school.

[2] Wagner, E., Jacques, D., Blake, W., and Pachter, M., 2002. "Flight test results of close formation flight for fuel savings". In AIAA Atmospheric Flight Mechanics Conference and Exhibit. AIAA-2002-4490.

[3] Tanner, H. G., and Christodoulakis, D. K., 2007. "Decentralized cooperative control of heterogeneous vehicle groups". *Robotics and autonomous systems,* **55**(11), pp. 811–823.

[4] Hedrick, J. K., Tomizuka, M., and Varaiya, P., 1994. "Control issues in automated highway systems". *IEEE Control Systems Magazine,* **14**, December, pp. 21 – 32.

[5] Zhang, Y., Kosmatopoulos, E. B., Ioannou, P. A., and Chien, C. C., 1999. "Autonomous intelligent cruise control using front and back information for tight vehicle following maneuvers". *IEEE Transactions on Vehicular Technology,* **48**, January, pp. 319–328.

[6] Jovanović, M. R., and Bamieh, B., 2005. "On the ill-posedness of certain vehicular platoon control problems". *IEEE Transactions on Automatic Control,* **50**(9), September, pp. 1307 – 1321.

[7] Barooah, P., Mehta, P. G., and Hespanha, J. P., 2009. "Mistuning-based decentralized control of vehicular platoons for improved closed loop stability". *IEEE Transactions on Automatic Control*. in press.

[8] Seiler, P., Pant, A., and Hedrick, J. K., 2004. "Disturbance propagation in vehicle strings". *IEEE Transactions on Automatic Control,* **49**, October, pp. 1835–1841.

[9] Yadlapalli, S. K., Darbha, S., and Rajagopal, K. R., 2006. "Information flow and its relation to stability of the motion of vehicles in a rigid formation". *IEEE Transactions on Automatic Control,* **51**(8), August.

[10] Barooah, P., and Hespanha, J. P., 2005. "Error amplification and disturbance propagation in vehicle strings". In Proceedings of the 44th IEEE conference on Decision and Control.

[11] Jovanović, M. R., Fowler, J. M., Bamieh, B., and D'Andrea, R., 2004. "On avoiding saturation in the control of vehicular platoons". In Proceedings of the 2004 American Control Conference, pp. 2257–2262.

[12] Fax, A. J., and Murray, R. M., 2004. "Information flow and cooperative control of vehicles". *IEEE Transactions on Automatic Control,* **49**, September, pp. 1465–1476.

[13] Barooah, P., and Hespanha, J. P., 2006. "Graph effective resistance and distributed control: Spectral properties and applications". In 45th IEEE Conference on Decision and Control, pp. 3479–3485.

[14] Bamieh, B., Jovanović, M. R., Mitra, P., and Patterson, S., 2008. "Effect of topological dimension on rigidity of vehicle formations: fundamental limitations of local feedback". In Proceedings of the 47th IEEE Conference on Decision and Control, pp. 369–374.